Journal of Materials Chemistry A

Accepted Manuscript

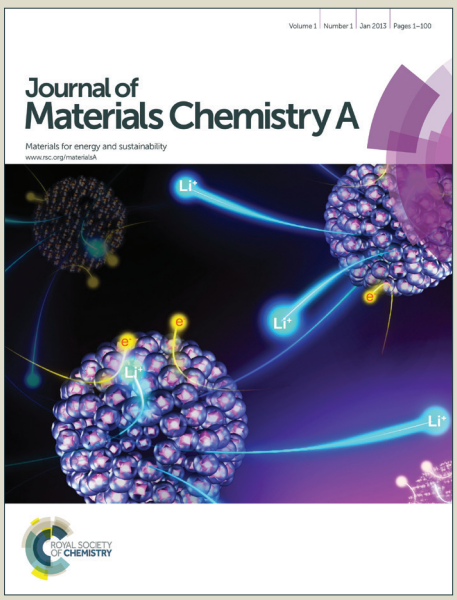

ROYAL SOCIETY OF CHEMISTRY

www.rsc.org/materialsA

Journal Name

RSCPublishing

ARTICLE

Preparation of 1D cubic $Cd_{0.8}Zn_{0.2}S$ solid solution nanowires using levelling effect of TGA and improved photocatalytic H_2-production activity

Cite this: DOI: 10.1039/x0xx00000x

Received 00th January 2012,
Accepted 00th January 2012

DOI: 10.1039/x0xx00000x

www.rsc.org/

Zhonghui Han, Gang Chen*, Chunmei Li, Yaoguang Yu, Yansong Zhou

The one-dimensional (1D) cubic $Cd_{0.8}Zn_{0.2}S$ solid solution nanowires are firstly prepared by the "levelling effect" of thioglycolic acid (TGA) at a solvothermal process. It exhibits the enhanced transfer and separation efficiency of carriers to improve the photocatalytic H_2-production activity. TGA not only serves as the sulphur source but also plays a template medium agent role. Furthermore, no selectivity of TGA for the diverse solvents to prepare 1D $Cd_{0.8}$ $Zn_{0.2}S$ solid solutions suggests it also may be extended to the preparation of other 1D metal sulphide solid solutions in the diverse solvents.

1 Introduction

Photocatalytic water splitting H_2 evolution is considered as an attractive approach to resolve the shortage problem of traditional energy source. In the past decades, the various visible-light-driven semiconductor photocatalysts have been developed for photocatalytic H_2 evolution.[1-8] Among them, the 1D nanomaterials have attracted widespread concerns due to their unique physical and chemical properties.[9-14] As the 1D nano-semiconductor photocatalysts, they can cause a dramatically change of band gap structure and the electron transition behaviour. The plenty of researches have reported that 1D nanostructure can significantly improve the photo-driving chemical reaction by adjusting the charge separation, transfer and the reaction process on the interfaces between photocatalyst and reactants.[10, 12, 15-17] Therefore, designing and developing novel 1D nanophotocatalysts is an effective and attractive preferred strategy to facilitate photocatalytic H_2 evolution.

In recent years, metal sulphides are considered as a kind of extraordinary candidates among the family of visible-light-driven photocatalysts.[18-20] CdS is a typical representative of the metal sulphides, which serving as the semiconductor photocatalyst has attracted key intention due to its narrowing band gap (2.4 eV) overlapping with the solar spectrum and high H_2-production activity.[21, 22] Yu and Weng reported the 1D CdS applied to the photocatalytic H_2 evolution, respectively, which is synthesized by the solvothermal method and exhibits an excellent photocatalytic water splitting H_2-production.[15, 23] For further improving photocatalytic activity, the various effective strategies have been successfully explored and developed.[18, 24-26] Recently, introducing zinc into CdS to form the $Cd_xZn_{1-x}S$ solid solution photocatalyst has been proved to be an effective method to improve the photocatalytic activity.[3, 27-29] For example, Wang and co-workers researched the $Cd_xZn_{1-x}S$ solid solutions prepared by the solvothermal method using ethylenediamine as the solvent and thiosemicarbazide as the sulphur source respectively, which displays an obviously improved H_2-production activity.[30] To our knowledge, most morphologies of the $Cd_xZn_{1-x}S$ solid solution photocatalyst reported is irregular particles and micro/nano-spheres. [31-34] In contrast, there are few reports about the preparation and photocatalytic activity of 1D $Cd_xZn_{1-x}S$ solid solutions. In fact, the 1D $Cd_xZn_{1-x}S$ solid solutions with large-ratio Zn content are hard to be prepared directly by a traditional technique owing to the discrepant physicochemical property of Cd^{2+} and Zn^{2+} ions. Therefore, if we explore a new organic agent which can eliminate the difference of physicochemical properties between Cd^{2+} and Zn^{2+} ions by forming metal organic complexes, the preparation of 1D $Cd_xZn_{1-x}S$ solid solution will be achievable.

TGA is an important bidentate ligand in the metal-organic chemistry, which can form four-coordinate metal-organic complexes by combining with the majority of metal ions because of its hydrosulphonyl (-SH) and carboxyl group (-COOH), similar to coprecipitation effect, which can result in a "levelling effect" to eliminate the difference of physicochemical properties of metal ions. These different four-coordinate metal complex molecules are more effortless to assemble the even-distributed 1D precursor *via* the dual hydrogen bonds between the sulfhydryl and carboxyl group at the specific hydrothermal/solvothermal conditions.

Hence, in our work, 1D cubic $Cd_{0.8}Zn_{0.2}S$ solid solution nanowires are prepared by the "levelling effect" of TGA at a solvothermal process for the very first time, which presents the improved photocatalytic H_2-prodction activity than 1D CdS and irregular cubic $Cd_{0.8}Zn_{0.2}S$ solid solution nanoparticles. In addition, formation mechanism of 1D cubic $Cd_{0.8}Zn_{0.2}S$ solid solution nanowires and the "levelling effect" of TGA are also discussed in detail.

2 Materials and methods

2.1 Chemicals

Chemical reagents including $Cd(CH_3COO)_2{\cdot}2H_2O$ (Aladding Chemistry Co. Ltd), $Zn(CH_3COO)_2{\cdot}2H_2O$ (Sinopharm Chemical Reagent Co., Ltd), thioglycolic acid (Aladding Chemistry Co. Ltd), were used without further treatment.

2.2 Preparation of $Cd_xZn_{1-x}S$ semiconductor samples

2.2.1 Preparation of 1D $Cd_{0.8}Zn_{0.2}S$ nanowires

In typical synthesis, 0.4264 g $Cd(CH_3COO)_2{\cdot}2H_2O$, 0.0878 g $Zn(CH_3COO)_2{\cdot}2H_2O$ and 32 mL N,N-Dimethylformamide (DMF) were added into Teflon-lined stainless steel. Then 0.1385 mL thioglycolic acid (TGA) was added into the solution following the mole ratio. The mixture reacted in autoclave at 140 °C for 8 h. The obtained production was washed twice with deionized water and ethanol separately. The time-dependent experiments were carried out at 1 h, 2 h, 4 h and 8 h. Other $Cd_xZn_{1-x}S$ samples were prepared based on different chemical mole ratio and remained other reaction conditions above.

2.2.2 Preparation of $Cd_{0.8}Zn_{0.2}S$ nanowires irregular particles

In typical synthesis, 0.4264 g $Cd(CH_3COO)_2{\cdot}2H_2O$, 0.0878 g $Zn(CH_3COO)_2{\cdot}2H_2O$ and 32 mL N,N-Dimethylformamide (DMF) were added into Teflon-lined stainless steel. Then 0.1385 mL thioglycolic acid (TGA) was added into the solution following the mole ratio. The mixture reacted in autoclave at 180 °C for 8 h. The obtained production was washed twice with deionized water and ethanol separately.

2.2.3 Preparation of precursor

$Cd(CH_3COO)_2{\cdot}2H_2O$ and $Zn(CH_3COO)_2{\cdot}2H_2O$ were dissolved in 32 mL DMF based on the mole ratio. Then TGA was added into the solution after $Cd(CH_3COO)_2{\cdot}2H_2O$ and $Zn(CH_3COO)_2{\cdot}2H_2O$ had dissolved completely. After the mixture was stirring for 5 min, the precursor is detached and washed by DMF and water separately for several times. The obtained product is dried and then solvothermal treated for 8 h in N,N-Dimethylformamide and deionized water at 140 °C separately.

2.3 Characterization:

The X-ray diffraction (XRD) patterns of the samples was obtained from 10 ° ～90 ° with the scanning step of 0.02 ° at the rate of 4 °/min using the Rigaku D/max-2000 X-ray diffractometer equipped with Cu kα radiation (λ=0.15406 nm). The capacity is 40 kV·50 mA. The element composition of the samples was determined by inductively coupled plasma emission spectrometry (ICP, Perkin Elmer Optima 5300DV) after the sample was dissolved in a mixture of HNO_3. The Camscan MX2600FE and the FEI Quanta 200FEG field emission scanning electron microscopy (FESEM) were used to characterize the morphology of the sample with the operating voltage of 20 kV. The transmission electron microscopy (TEM) and the high-resolution TEM (HR-TEM) of the hierarchical structures of the samples were analysed through the FEI Tecnai G2 F30 operating at 300 kV. UV-vis diffuse reflectance spectra were detected by a spectrophotometer (TU-1900) and the reflectance standard used was $BaSO_4$. The reflection was converted to absorbance by the standard Kubelka–Munk method.

2.4 Photocatalytic reactions:

The photocatalytic reactions were carried out in a closed gas circulation system. The photocatalyst powder was homogeneously dispersed by ultrasonic for 0.5~1 h into 300 mL aqueous with 0.8 M Na_2S and 0.6 M Na_2SO_3 as sacrifice agents. The as prepared solution containing photocatalyst powder was performed the photocatalytic reaction at 287 K under the irradiation of a 300 W xenon lamp (Trusttech PLS-SXE 300, Beijing) with an optical filter (λ>400 nm) from the side window. The amount of H_2 was measured by the gas chromatography (Agilent 6820) with a thermal conductivity detector (TCD) and Ar was used as the carrier gas.

2.5 Photoelectrochemical measurements

The photoelectrochemical characteristics are evaluated using a standard three-compartment cell via a CHI604C electrochemical working station. 0.05g photocatalyst powder was ground with 0.5 mL terpilenol together for 20min and spin-coated onto FTO glass. The sample coated FTO glass was dried at 90 °C for 12 h. Catalyst coated FTO glass, a piece of Pt sheet, a Ag/AgCl electrode and 0.8 M Na_2S and 0.6 M Na_2SO_3 are used as the working electrode, count electrode, reference electrode and electrolyte, respectively

3 Results and discussion

The Cd: Zn ratio obtained by inductively coupled plasma (ICP) elemental analysis is 0.81:0.21, which is closed to the mole ratio of metal anion in the reactant solution. The crystal structure and phase composition of $Cd_{0.8}Zn_{0.2}S$ solid solutions are investigated by XRD. From the XRD patterns, both samples obtained at 140 °C (Fig. 1) and 180 °C (Fig. S1) share the same cubic phase, all diffraction peaks are indexed the cubic CdS crystal phase and match with the (111), (220) and (311) crystal plane, respectively. They display a slight shift to the high diffraction angle compared with the standard diffraction pattern (JCPDS No. 75-1546) and pure CdS prepared through the same route, which results from the interplanar crystal spacing reduction owing to the zinc atoms into the CdS. Interestingly, the diffraction intensity of (111) crystal plane is much higher

than that of (220) and (311) crystal plane relative to the standard diffraction pattern, suggesting the crystal may be inclined to grow along the (111) direction.[35]

The morphology of as-prepared cubic $Cd_{0.8}Zn_{0.2}S$ solid solution is also investigated by FESEM and TEM (Fig. 2).

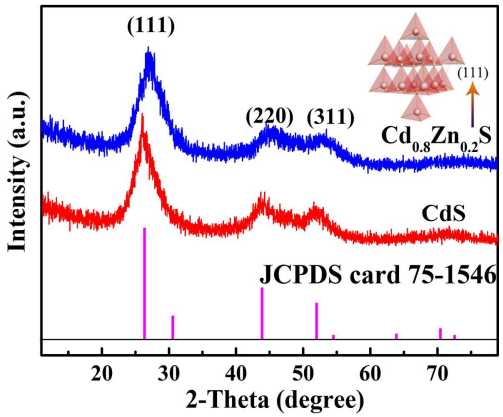

Fig.1 XRD pattern of the as-prepared $Cd_{0.8}Zn_{0.2}S$ solid solution sample.

From the FESEM image in Fig. 2a, the sample obtained at 140 °C appears a uniform 1D nanowire feature compared to the irregular particles morphology of the sample obtained at 180 °C (Fig S2). These 1D nanowires exhibit a large length-to-diameter ratio with the length ranges from hundreds of nanometres to several micrometres and the diameters of ~30 nm. The microstructure characteristics of the 1D cubic $Cd_{0.8}Zn_{0.2}S$ solid solution nanowires are analysed by TEM and HRTEM. The HRTEM image in Fig. 2b further identifies the formation of 1D cubic $Cd_{0.8}Zn_{0.2}S$ solid solution nanowires in accord with the results revealed by FESEM. It is worth noting that the single 1D nanowire appears to be prismatic instead of cylindrical corresponding the TEM images with the angle rotation in Fig. 2d-e confirm the existence of the distinct edge. In addition, the selected area electron diffraction (SAED) is performed on a single cubic $Cd_{0.8}Zn_{0.2}S$ solid solution nanowire in Fig. 2b, in which the generated diffraction ring patterns demonstrate the as-prepared sample is polycrystalline and derive from (111), (220) and (311) crystal planes of cubic CdS, respectively. The polycrystalline structure feature is also confirmed by some emerged crystal domains with the different crystal orientations in HRTEM image (Fig. 2f). These crystal domains have a same interplanar crystal spacing of ~0.334 nm, which is agree well with the (111) crystal plane of cubic CdS. All above prove that the 1D cubic $Cd_{0.8}Zn_{0.2}S$ solid solution nanowires are successfully obtained by the "levelling effect" of TGA at a facile solvothermal process.

The formation mechanism of 1D cubic $Cd_{0.8}Zn_{0.2}S$ solid solution nanowires is further explored by the time-dependent experiment. Fig. 3 shows the FESEM images of the sample evolved over time. After reacting 1 h (Fig. 3a), the obtained sample exhibits the irregular nanoparticle shapes with diameter of ~60 nm. When the reaction processes to 2 h (Fig. 3b), the irregular nanoparticles grow bigger and longer but no 1D morphology sample appears. Further proceeding reaction to 4 h

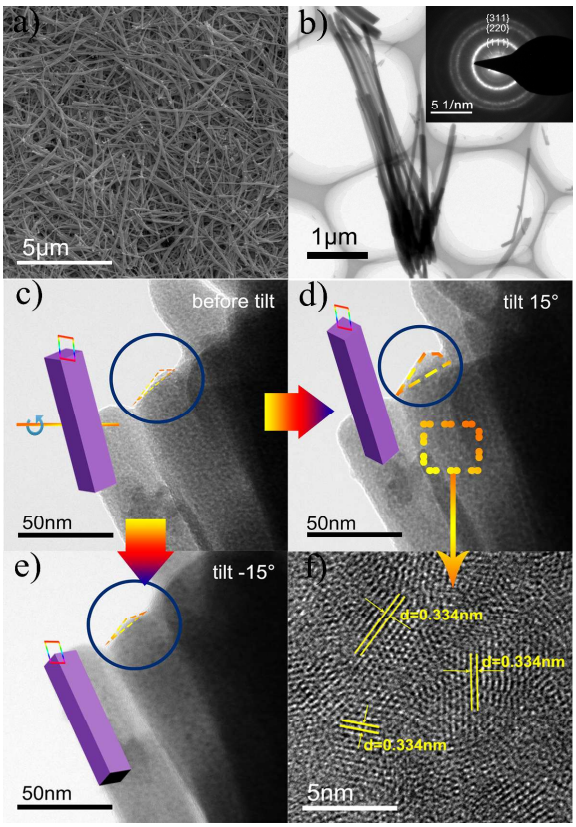

Fig.2 SEM image (a), TEM image (b), SAED image (inset) of the as-prepared $Cd_{0.8}Zn_{0.2}S$ solid solution. TEM images with rotation angle (c-e) and HR-TEM image (f).

(Fig. 3c), 1D nanorods appear in large numbers, and the amount of irregular nanoparticles decrease obviously. When the reaction is carried out for 8h (Fig. 3d), the length of 1D

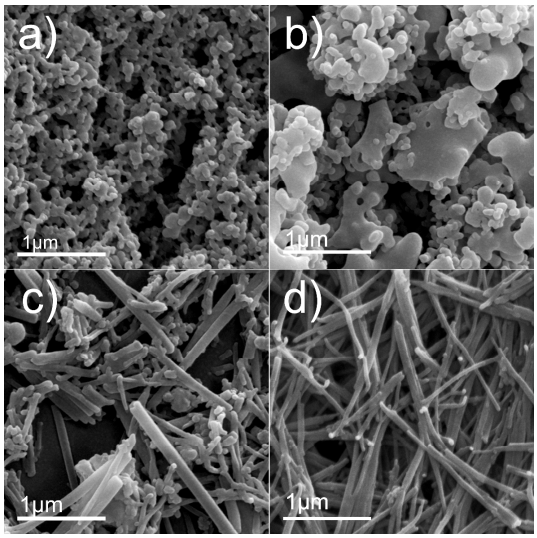

Fig. 3 SEM images of the $Cd_{0.8}Zn_{0.2}S$ samples with different reaction time variation, 1h (a), 2h (b), 4h (c) and 8h (d).

nanorods are clearly longer and transform into nanowires, which are bend and decrease in the diameters obviously. We note that the variation from the nanorods to nanowires between

4 h and 8 h seem to be more arresting, which implies it may be decomposition process of TGA-precursor containing Cd^{2+}/Zn^{2+} ions. This result is evidenced by the XRD of the sample obtained at 4 h to 8 h in Fig. 4. Compared with the pure sample

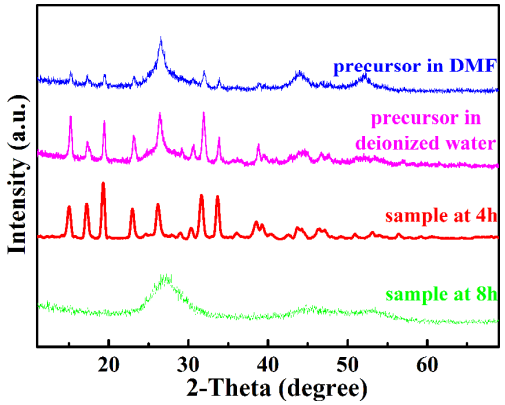

Fig.4 XRD patterns of the precursor solvothermal treated in DMF and deionized water, and the as-prepared samples.

obtained at 8 h, the diffraction peaks of unknown phase is observed in XRD of the sample obtained at 4 h besides that of cubic $Cd_{0.8}Zn_{0.2}S$ solid solutions, which may be the generated TGA-precursor containing Cd^{2+}/Zn^{2+} ions at the reaction process. To confirm the formation of the TGA-precursor containing Cd^{2+}/Zn^{2+} ions, it is synthesized particularly and solvothermal treated in DMF and deionized water separately. The XRD patterns of two precursors are shown in Fig. 4, which match well with that of the sample prepared at 4h. It attests that the generation of TGA-precursor containing Cd^{2+}/Zn^{2+} ions at the formation process of 1D $Cd_{0.8}Zn_{0.2}S$ solid solution nanowires. In addition, from the corresponding SEM images in Fig. 5a-b, it is clear that two precursors all have the 1D nanorods morphology. Based on above analyses, thus, the formation mechanism of 1D $Cd_{0.8}Zn_{0.2}S$ solid solution nanowires involves two key steps, concluding the generation and decomposition of 1D nanorod TGA-precursors containing Cd^{2+}/Zn^{2+} ions. We know that TGA is a typical bidentate ligand in the metal-organic chemistry, which can combine with most metal ions by ligand bonds owing to hydrosulphonyl (-SH) and carboxyl group (-COOH) in its molecular. Therefore, metal-

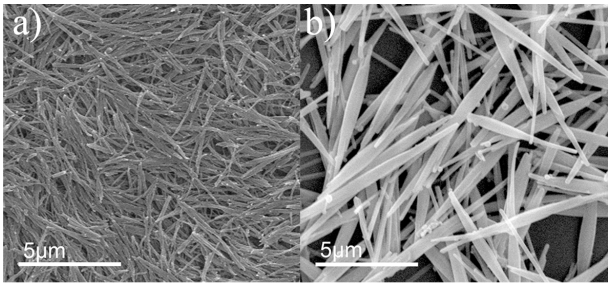

Fig.5 SEM images of the precursors solvothermal treated in DMF (a) and deionized water (b).

organic complexes Cd^{2+}/Zn^{2+}-TGA are quickly produced when TGA are add into the Cd^{2+}/Zn^{2+} ions solutions. According to the ligand field theory, a Cd^{2+}/Zn^{2+} ion tends to combine with two TGA molecules and form a four-coordinated metal-organic complex with tetrahedral configuration, in which Cd^{2+}/Zn^{2+} ion and oxygen/sulphur in TGA occupy the centre of the tetrahedron and four vertexes, respectively. For one thing, similar to co-precipitation effect, the formation of complexes can result in a "levelling effect" to eliminate the difference of physicochemical properties of Cd^{2+}/Zn^{2+} ions. The other hand, the unique coordination mode of complex molecules can form the dual hydrogen bonds between the sulfhydryl and carboxyl group at the specific solvothermal conditions, which can more effective to assemble the even-distributed 1D TGA-precursor containing Cd^{2+}/Zn^{2+} ions.

Based on above analyses, a feasible mechanism is raised and displayed in Scheme 1. We here should point out TGA play

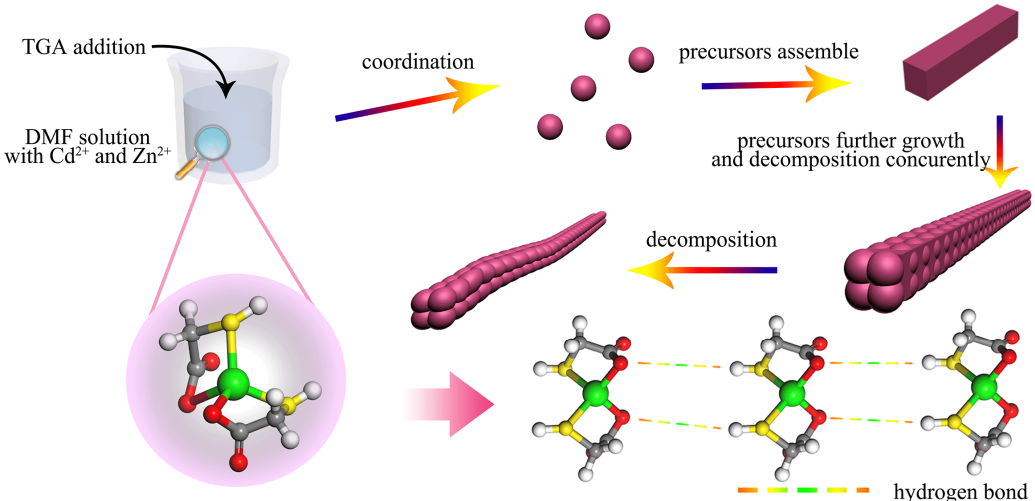

Scheme 1 Growth mechanism of the 1D $Cd_{0.8}Zn_{0.2}S$ solid solution nanowires.

two important roles in the solvothermal process, which serves as both the sulphur source and template agent. First is the generation of 1D TGA-precursor nanorods containing Cd^{2+}/Zn^{2+} ions. When TGA and reaction raw materials are added into DMF solvent, the plenty of precursor nanoparticles are produced. With the hydrothermal reaction processing, the precursor nanoparticles can take place the dissolving-recrystallizing process. Meanwhile, most Cd^{2+}/Zn^{2+}-TGA complex molecules connect with each other via the double hydrogen bonds produced between its own sulfhydryl and carboxyl, thus generating the 1D TGA-precursor nanorods containing Cd^{2+}/Zn^{2+} ions. Second is the generation of 1D cubic $Cd_{0.8}Zn_{0.2}S$ solid solution nanowires. As continuing to prolong ligand field theory, a Cd^{2+}/Zn^{2+} ion tends to combine with two TGA molecules and form a four-coordinated metal-organic reaction times, the 1D TGA-precursor nanorods containing Cd^{2+}/Zn^{2+} ions further grow longer and slowly decompose to release the S ions that recombine with Cd^{2+}/Zn^{2+} ions, finally forming 1D cubic $Cd_{0.8}Zn_{0.2}S$ solid solution nanowires.

To further confirm the universal "levelling effect" of TGA in the preparation of 1D cubic $Cd_{0.8}Zn_{0.2}S$ solid solution nanowires, the different solvents are applied to prepare the sample with 1D morphology under the same conditions. As can be seen form the FESEM images in Fig. 6, the samples prepared in pyridine, tetrahydrofuran (THF), ethylenediamine (EDA) solvents all display an analogous 1D morphology characteristic. We note that the limited nanoparticles are also produced in the FESEM images in Fig. 6. This may be due to the different growth and decomposition speed of the TGA-precursor nanorods containing Cd^{2+}/Zn^{2+} ions in the different solvents. Despite all this, the same trend forming 1D morphology indicates that the "levelling effect" has almost no selectivity to the different solvents. Furthermore, TGA is a universal sulphur source to prepare 1D metal sulphide nanorods/nanowires in the diverse solvents.

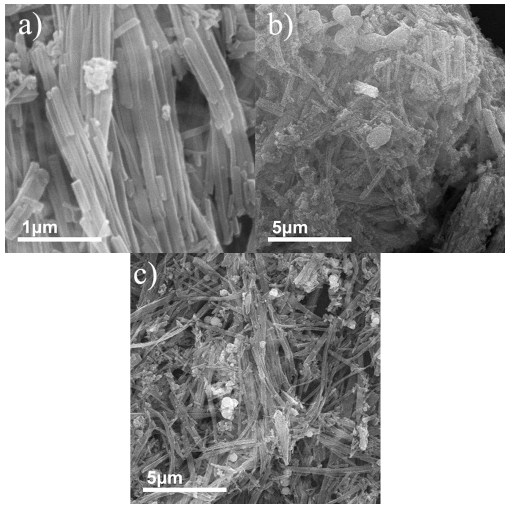

Fig. 6 SEM images of the as-prepared $Cd_{0.8}Zn_{0.2}S$ solid solution in different solvents, (a) pyridine, (b) THF and (c) EDA.

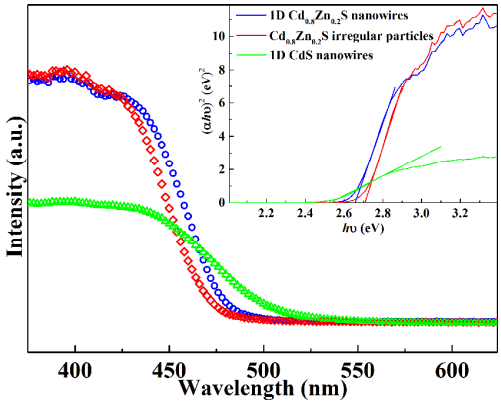

Fig. 7 UV-vis diffuse reflectance spectra and $(\alpha h\nu)^2$ vs. $h\nu$ plots (inset) of different samples.

Moreover, the effects of 1D morphology feature on the light absorption of cubic $Cd_{0.8}Zn_{0.2}S$ solid solution are evaluated by UV-Vis DRS. As shown in Fig. 7, the absorption edges of cubic $Cd_{0.8}Zn_{0.2}S$ solid solutions are less than that of1D CdS owing to the introduction of Zn into CdS. [36, 37] It is noticed that the light harvest ability of the 1D cubic $Cd_{0.8}Zn_{0.2}S$ solid solution nanowires is obviously higher than that the cubic $Cd_{0.8}Zn_{0.2}S$ solid solution nanoparticles because the absorption edge of former exhibits a distinct red-shift compared with the latter. According to the empirical equation $\alpha h\nu = A(h\nu - E_g)^n$ [38, 39], we plot $(\alpha h\nu)^2$ versus $h\nu$ and obtain that band gap values of 1D cubic $Cd_{0.8}Zn_{0.2}S$ solid solution nanowires and cubic $Cd_{0.8}Zn_{0.2}S$ solid solution nanoparticles are 2.65 eV and 2.71 eV, respectively. It demonstrates that 1D cubic $Cd_{0.8}Zn_{0.2}S$ solid solution nanowires are conducive to excitation of electrons from the valence band to conduction band for improving the photocatalytic activity[40-42].

The photocurrent responses of the samples are also carried out. From Fig. 8, the cubic $Cd_{0.8}Zn_{0.2}S$ solid solutions all exhibit the more intense photocurrent responses than 1D CdS at the same bias voltage. It is worth noting that the photocurrent response of 1D cubic $Cd_{0.8}Zn_{0.2}S$ solid solution nanowires electrode is obviously higher than that the cubic $Cd_{0.8}Zn_{0.2}S$ solid solution nanoparticles electrode, which indicates that the former has more superior charge carriers separation efficiency and faster charge transfer through the electrode interface.[38, 43-45] It contributes to increasing the photocatalytic activity of the photocatalyst on water splitting hydrogen evolution. In addition, the diameters of 1D cubic $Cd_{0.8}Zn_{0.2}S$ solid solution nanowires are smaller than that of cubic $Cd_{0.8}Zn_{0.2}S$ solid solution particles. The reduction of the diameter may cause the decreasing of high-angle grain boundaries along the direction of photogenerated charge transport, thus causing a stronger charge transmission capability.[46]

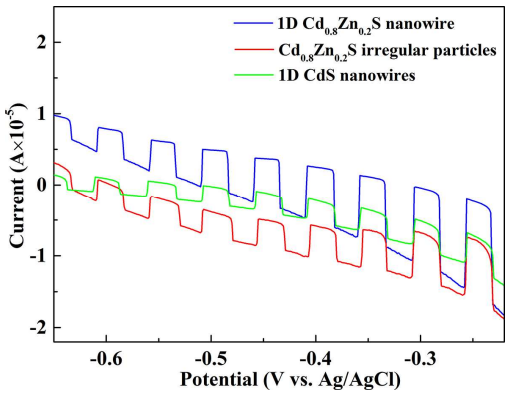

Fig. 8 Photocurrent response of 1D nanorods $Cd_{0.8}Zn_{0.2}S$ electrode and irregular particle electrode.

The photocatalytic H_2 evolution from water splitting are carried out to evaluate the activities of the as-prepared sample with different morphology. Fig. 9 shows that all the $Cd_{0.8}Zn_{0.2}S$ solid solutions exhibit the higher H_2-production activity than that of 1D CdS (52.3μmol·h^{-1}). In addition, the photocatalytic activities of $Cd_{0.8}Zn_{0.2}S$ solid solutions with 1D morphology prepared in the different solvents are also 50% more superior to the $Cd_{0.8}Zn_{0.2}S$ solid solution nanoparticles. Especially for 1D cubic $Cd_{0.8}Zn_{0.2}S$ solid solution nanowires obtained in the DMF solvent, the H_2-production rate reaches to 157.46 μmol·h^{-1} which is the 6.32%, 8.36% and 14.81% times more than that of the samples prepared in pyridine (148.1 μmol·h^{-1}), THF (145.3 μmol·h^{-1}) and EDA (137.1 μmol·h^{-1}) solvents. It may be result from the larger ratio of length-to-diameter of polycrystalline 1D cubic $Cd_{0.8}Zn_{0.2}S$ solid solution nanowires that can provide more active sites.[47] Even after recycling for 12 h, the hydrogen

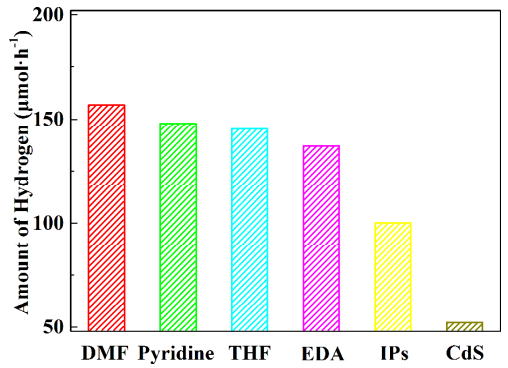

Fig. 9 Rates of photo-driven water splitting H_2 evolution of different samples

production still reaches to 40.2μmol·h^{-1} (Fig. S3). The decrease in photocatalytic activity of the 1D cubic $Cd_{0.8}Zn_{0.2}S$ solid solution nanowires is contributed to its photocorrosion confirmed by the XRD pattern of the sample after cycling 12 h (Fig. S4). In addition, the photocatalytic activities of the $Cd_xZn_{1-x}S$ (x=1, 0.8, 0.6, 0.4, 0.2) were measured (Fig. S5). The results show the outstanding photocatalytic performance of the $Cd_{0.8}Zn_{0.2}S$ compared to other samples with different Cd-Zn ratio.

Conclusion

In summary, the uniform 1D cubic $Cd_{0.8}Zn_{0.2}S$ solid solution nanowires with large length-diameter ratio is prepared by a solvothermal reaction, which enhance the transfer and separation efficiency of carriers, improving photocatalytic H_2-production activity. TGA play two important roles in the solvothermal process, which serves as both the sulphur source and template agent. The unique bidentate ligand structure can coordinate with Cd^{2+}/Zn^{2+} ions to produce metal organic complexes and induce these complex molecules to form 1D TGA-precursor containing Cd^{2+}/Zn^{2+} ions nanorods via dual hydrogen-bond interaction, finally releasing S ions that recombine with Cd^{2+}/Zn^{2+} ions to generate 1D cubic $Cd_{0.8}Zn_{0.2}S$ solid solution nanowires. In addition, TGA has no selectivity for the diverse solvents to prepare the $Cd_{0.8}Zn_{0.2}S$ solid solutions with 1D morphology, which implies it may be applied to prepare other 1D metal sulphide solid solutions in the different solvents.

Acknowledgements

This work was financially supported by projects of Natural Science Foundation of China (21271055 and 21471040), the Fundamental Research Funds for the Central Universities (HIT. IBRSEM. A. 201410). We acknowledge for the support by Open Project of State Key Laboratory of Urban Water Resource and Environment, Harbin Institute of Technology (No.QAK201304) and Program for Innovation Research of Science in Harbin Institute of Technology (PIRS of HIT B201412).

Notes and references

Department of Chemistry, Harbin Institute of Technology, Harbin 150001, P. R. China. E-mail: gchen@hit.edu.cn

Electronic Supplementary Information (ESI) available: XRD pattern of the as prepared $Cd_{0.8}Zn_{0.2}S$ solid solution at 180 °C (Fig. S1); SEM image of the as prepared $Cd_{0.8}Zn_{0.2}S$ solid solution at 180 °C (Fig. S2); Cycle operation of H_2 evolution on the as-prepared 1D $Cd_{0.8}Zn_{0.2}S$ solid solution nanowires (Fig. S3); XRD pattern of the 1D $Cd_{0.8}Zn_{0.2}S$ solid solution nanowires after cycling for 12 h (Fig. S4); Photocatalytic activities of the $Cd_xZn_{1-x}S$ with different Cd-Zn ratio, x=1, 0.8, 0.6, 0.4, 0.2 (Fig. S5). See DOI: 10.1039/b000000x/

1. I. Tsuji, H. Kato, H. Kobayashi and A. Kudo, *J. Am. Chem. Soc.*, 2004, **126**, 13406.
2. C. G. Silva, R. Juarez, T. Marino, R. Molinari and H. Garcia, *J. Am. Chem. Soc.*, 2011, **133**, 595.
3. J. Zhang, J. Yu, M. Jaroniec and J. R. Gong, *Nano lett.*, 2012, **12**, 4584.
4. M. Elvington, J. Brown, S. M. Arachchige and K. J. Brewer, *J. Am. Chem. Soc.*, 2007, **129**, 10644.
5. I. Tsuji, H. Kato, H. Kobayashi and A. Kudo, *J. Phys. Chem. B*, 2005, **109**, 7323.
6. I. Tsuji, H. Kato and A. Kudo, *Chem. Mater.*, 2006, **18**, 1969.

7. F. He, G. Chen, Y. Yu, S. Hao, Y. Zhou and Y. Zheng, *ACS Appl. Mater. Inter.*, 2014, 6, 7171.
8. Y. Wang, X. Wang and M. Antonietti, *Angew. Chem. Int. Edit*, 2012, 51, 68.
9. Y. Xia, P. Yang, Y. Sun, Y. Wu, B. Mayers, B. Gates, Y. Yin, F. Kim and H. Yan, *Adv. Mater.*, 2003, **15**, 353.
10. Z. Tang and N. A. Kotov, *Adv. Mater.*, 2005, **17**, 951.
11. T. Yang, H. Wang, X. M. Ou, C. S. Lee and X. H. Zhang, *Adv. Mater.*, 2012, **24**, 6199.
12. T. Zhu, H. B. Wu, Y. Wang, R. Xu and X. W. Lou, *Adv. Energy Mater.*, 2012, **2**, 1497.
13. F. Dong, W. Zhao and Z. Wu, *Nanotechnology*, 2008, **19**, 365607.
14. X. Zhou, H. Yang, C. Wang, X. Mao, Y. Wang, Y. Yang and G. Liu, *J. Phys. Chem. C*, 2010, **114**, 17051.
15. J. Yu, Y. Yu, P. Zhou, W. Xiao and B. Cheng, *App. Catal. B-Environ.*, 2014, **156-157**, 184.
16. B. Weng, S. Liu, Z.-R. Tang and Y.-J. Xu, *RSC Adv.*, 2014, **4**, 12685.
17. L. Wang, H. Wei, Y. Fan, X. Gu and J. Zhan, *J. Phys. Chem. C*, 2009, **113**, 14119.
18. D. Jing and L. Guo, *J. Phys. Chem. B*, 2006, **110**, 11139.
19. I. Tsuji, Y. Shimodaira, H. Kato, H. Kobayashi and A. Kudo, *Chem. Mater.*, 2010, **22**, 1402.
20. H. Kaga, K. Saito and A. Kudo, *Chem. Commun.*, 2010, **46**, 37791.
21. X. Zong, H. Yan, G. Wu, G. Ma, F. Wen, L. Wang and C. Li, *J. Am. Chem. Soc.*, 2008, **130**, 7176.
22. N. Bao, L. Shen, T. Takata and K. Domen, *Chem. Mater.*, 2007, **20**, 110
23. J. Jin, J. Yu, G. Liu and P. K. Wong, *J. Mater. Chem. A*, 2013, **1**, 10927.
24. H. Yan, J. Yang, G. Ma, G. Wu, X. Zong, Z. Lei, J. Shi and C. Li, *J. Catal.*, 2009, **266**, 165.
25. L. Amirav and A. P. Alivisatos, *J. Phys. Chem. Lett.*, 2010, **1**, 1051.
26. J. S. Jang, U. A. Joshi and J. S. Lee, *J. Phys. Chem. C*, 2007, **111**, 13280.
27. Q. Li, H. Meng, P. Zhou, Y. Zheng, J. Wang, J. Yu and J. Gong, *ACS Catal.*, 2013, **3**, 882.
28. W. Li, D. Li, W. Zhang, Y. Hu, Y. He and X. Fu, *J. Phys. Chem. C*, 2010, **114**, 2154.
29. Y. G. Yu, G. Chen, L. X. Hao, Y. S. Zhou, Y. Wang, J. Pei, J. X. Sun and Z. H. Han, *Chem. Commun.*, 2013, **49**, 10142.
30. L. Wang, Y. Jiang, C. Wang, W. Wang, B. Cao, M. Niu and Y. Qian, *J. Alloy. Compd.*, 2008, **454**, 255.
31. W. Wang, W. Zhu and H. Xu, *J. Phys. Chem. C*, 2008, **112**, 16754.
32. G. Yellaiah, K. Hadasa and M. Nagabhushanam, *J. Cryst. Growth*, 2014, **386**, 62.
33. W. Li, D. Li, Z. Chen, H. Huang, M. Sun, Y. He and X. Fu, *The J. Phys. Chem. C*, 2008, **112**, 14943.
34. X. Xu, R. Lu, X. Zhao, Y. Zhu, S. Xu and F. Zhang, *App. Catal. B-Environ.*, 2012, **125**, 11.
35. P. Yang, H. Yan, S. Mao, R. Russo, J. Johnson, R. Saykally, N. Morris, J. Pham, R. He and H. J. Choi, *Adv. Funct. Mater.*, 2002, **12**, 323.
36. J. Wang, P. Yang, J. Zhao and Z. Zhu, *App. Surf. Sci.*, 2013, **282**, 930.
37. J. Shi, H. n. Cui, Z. Liang, X. Lu, Y. Tong, C. Su and H. Liu, *Energy & Environ. Sci.*, 2011, **4**, 466.
38. H. Dong, G. Chen, J. Sun, Y. Feng, C. Li and C. Lv, *Chem. Comm.*, 2014, **50**, 6596.
39. L. Shang, C. Zhou, T. Bian, H. Yu, L.-Z. Wu, C.-H. Tung and T. Zhang, *J. Mater. Chem. A*, 2013, **1**, 4552.
40. C. Li, G. Chen, J. Sun, H. Dong, Y. Wang and C. Lv, *App. Catal. B-Environ.*, 2014, **160–161**, 383.
41. M. Wang, L. Sun, J. Cai, P. Huang, Y. Su and C. Lin, *J. Mater. Chem. A*, 2013, **1**, 12082.
42. Y. Yu, J. Zhang, X. Wu, W. Zhao and B. Zhang, *Angew. Chem.*, 2012, **51**, 897.
43. C. Li, G. Chen, J. Sun, Y. Feng, J. Liu and H. Dong, *App. Catal. B-Environ.*, 2015, **163**, 415.
44. Q. Kang, J. Cao, Y. Zhang, L. Liu, H. Xu and J. Ye, *J. Mater. Chem. A*, 2013, **1**, 5766.
45. J. Yu, J. Jin, B. Cheng and M. Jaroniec, *J. Mater. Chem. A*, 2014, **2**, 3407.
46. S. C. Warren, K. Voïtchovsky, H. Dotan, C. M. Leroy, M. Cornuz, F. Stellacci, C. Hébert, A. Rothschild and M. Grätzel, *Nat. Mater.*, 2013, **12**, 842.
47. Y. F. Li and Z. P. Liu, *J. Am. Chem. Soc.*, 2011, **133**, 15743.

Graphic abstract

The one-dimensional (1D) cubic $Cd_{0.8}Zn_{0.2}S$ solid solution nanowires prepared based on the "levelling effect" of thioglycolic acid (TGA). It exhibits enhanced photocatalytic H_2-production activity.